TRANSIENT SURFACE ELASTIC WAVES IN COATING-SUBSTRATE ANISOTROPIC MATERIALS

O. Poncelet, H. Meri, M. Deschamps and B. Audoin
Laboratoire de Mécanique Physique UMR CNRS 5469, Université Bordeaux 1, Bordeaux
o.poncelet@lmp.u-bordeaux1.fr

Abstract

Calculation of the elastodynamic response of an anisotropic coated-substrate to an impulsive localized source is performed by means of generalized-ray theory and Cagniard-de Hoop method. Resulting time-space Green's function is composed of different wave constituent contributions stemming from multiple mode conversions at interfaces. Combining both generalized-ray approach and Cagniard technique leads to a comprehensive understanding of calculated signals in the time domain, in terms of bulk wave arrivals, interface and bulk diffraction features (head-waves and cusp focusing). The proposed results exemplify those phenomena and give a picture of the perturbation of the transient Rayleigh wave at the free surface of the coating due to the substrate.

Introduction

In laser-ultrasonics NDE of coated anisotropic materials, many devices involve very short pulses (a few nanoseconds and even less nowadays), line-like sources and point receivers. Experimental waveforms are therefore often comparable to theoretical Green's functions and a good understanding of the acquired signals is then very important, especially for highly anisotropic layers. This work deals with the elastodynamic 2D space-time response of an anisotropic layer upon a substrate to a transient line-force on the free surface. Abilities of the Cagniard-de Hoop method for evaluating solution back to the physical space is used. Contrary to others methods that require either restrictive hypothesis such as, a high frequency content or a long distance propagation, or necessitate purely numerical lengthy computation, the generalized-ray theory associated with Cagniard technique is a very good candidate for obtaining exact solutions in the space-time domain without any kind of restrictions and for a wide class of anisotropic materials [1].

Basic Equations

The figure 1 shows the configuration of the problem. The direction x_3 is normal to the interfaces delimiting the coating of thickness h. The line-source of vertical force acting at the upper surface of the structure is orthogonal to the plane (x_1,x_3) which is a plane of symmetry of both the layer (medium 1) and the substrate (medium 2). The plane (x_1,x_2) is also a plane of symmetry for the media.

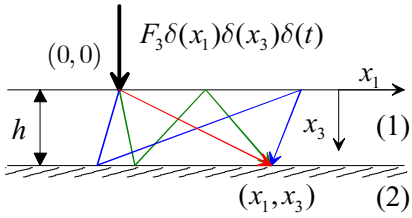

Figure 1: Coating-substrate medium

The equations of motion for the displacement field $u_i(x_1,x_3,t)$ in medium (1) and (2) are given by:

$$c_{ijkl}^{(m)}\partial_j\partial_k u_l - \rho^{(m)}\partial_t^2 u_i = 0\,, \qquad (1)$$

where $c_{ijkl}^{(m)}$ is the stiffness tensor of rank 4 and $\rho^{(m)}$ the mass density of medium (m). All following considerations apply for wave field in both media. In order to present solution concisely and because we are mainly interested in the surface response, derivation is presented only for the coating, and unless mentioned, the superscript referring to the medium is omitted. We seek solutions for u_i in the Fourier-Laplace domain. The Laplace transform is defined by:

$$\hat{u}_i(x_1,x_3,p) = \int_0^{+\infty} u_i(x_1,x_3,t)e^{-pt}dt\,, \qquad (2)$$

and the Fourier-Laplace transform of u_i takes the form:

$$\tilde{u}_i(x_3,s_1,p) = \int_{-\infty}^{+\infty} \hat{u}_i(x_1,x_3,p)e^{ps_1x_1}dx_1\,. \qquad (3)$$

The solutions in terms of plane waves of the transformed equations of motion are:

$$\tilde{u}_i^{(\pm n)}(x_3,s_1,p) = a^{(\pm n)}P_i^{(\pm n)}e^{-ps_3^{(\pm n)}x_3}\,, \qquad (4)$$

in which the slownesses $(s_1,s_3(s_1))$ and the polarization P_i verify the eigenvalue problem of Christoffel. The solutions are labelled by $\pm n$ that expresses the quasi-longitudinal ($n=1$ or $n=L$) and the quasi-transversal ($n=2$ or $n=T$) type of the partial plane wave. The signs + and - stand for the down and up-going waves respectively. Note that due to the symmetry of the medium, the vertical slownesses of up and down-going plane waves are such that: $s_3^{(-1)} = -s_3^{(+1)}$ and $s_3^{(-2)} = -s_3^{(+2)}$. In the transform domain, the boundary conditions that take into account the loaded upper interface and continuity of wave field at the second interface are: $\tilde{\sigma}_{33}(x_3=0) = F_3$, $\tilde{\sigma}_{13}(x_3=0) = 0$; $\tilde{\sigma}_{33}$, $\tilde{\sigma}_{13}$ and $\tilde{u}_i$ continuous across $x_3 = h$. The amplitudes $a^{(\pm n)}$ (of partial waves in the layer) and $b^{(+n)}$ (of waves in the substrate) are found by solving the 6x6 linear system:

$$AX = S\,, \qquad (5)$$

where $X=(a^{(+1)},a^{(+2)},a^{(-1)}e^{-ps_3^{(-1)}h},a^{(-2)}e^{-ps_3^{(-2)}h},$ $b^{(+1)}e^{-pq_3^{(+1)}h},b^{(+2)}e^{-pq_3^{(+2)}h})^T$ is the vector of unknown amplitudes and $q_3^{(+n)}$ the vertical slownesses in the substrate. The vector $S=(F_3,0,0,0,0,0)^T$ is the source term and the matrix A is composed of the column-vectors of the partial vertical stresses and displacement due to each wave, expressing boundary conditions:

$$A=\begin{pmatrix} \tilde{\sigma}_{33}^{+1} & \tilde{\sigma}_{33}^{+2} & \tilde{\sigma}_{33}^{-1}e^{ps_3^{-1}h} & \tilde{\sigma}_{33}^{-2}e^{ps_3^{-2}h} & 0 & 0 \\ \tilde{\sigma}_{13}^{+1} & \tilde{\sigma}_{13}^{+2} & \tilde{\sigma}_{13}^{-1}e^{ps_3^{-1}h} & \tilde{\sigma}_{13}^{-2}e^{ps_3^{-2}h} & 0 & 0 \\ \tilde{\sigma}_{33}^{+1}e^{-ps_3^{+1}h} & \tilde{\sigma}_{33}^{+2}e^{-ps_3^{+2}h} & \tilde{\sigma}_{33}^{-1} & \tilde{\sigma}_{33}^{-2} & \tilde{\sigma}_{33}^{+1} & \tilde{\sigma}_{33}^{+2} \\ \tilde{\sigma}_{13}^{+1}e^{-ps_3^{+1}h} & \tilde{\sigma}_{13}^{+2}e^{-ps_3^{+2}h} & \tilde{\sigma}_{13}^{-1} & \tilde{\sigma}_{13}^{-2} & \tilde{\sigma}_{13}^{+1} & \tilde{\sigma}_{13}^{+2} \\ P_1^{+1}e^{-ps_3^{+1}h} & P_1^{+2}e^{-ps_3^{+2}h} & P_1^{-1} & P_1^{-2} & \xi_1^{+1} & \xi_1^{+2} \\ P_3^{+1}e^{-ps_3^{+1}h} & P_3^{+2}e^{-ps_3^{+2}h} & P_3^{-1} & P_3^{-2} & \xi_3^{+1} & \xi_3^{+2} \end{pmatrix}$$

Partial stress takes the form $\tilde{\sigma}_{i3}^{(\pm n)}=-pc_{i3kl}^{(1)}s_k^{(\pm n)}P_l^{(\pm n)}$ and $\tilde{\sigma}_{i3}^{(+n)}=-pc_{i3kl}^{(2)}q_k^{(+n)}\xi_l^{(+n)}$, for the layer and the substrate respectively. The vector amplitude X, solution of the system (5), is frequency dependent due to the different phase terms and account for global wave interactions through the plate. In view of obtaining explicit time-solution in terms of ray paths and wave arrivals, we may rewrite the system (5) into a formulation which separates phase terms due to propagation in the layer, from the reflection terms at the interfaces, that are frequency independent. By setting $A=M+B$, where M (including no phase terms) and B are constituted of 2x2 and 4x4 block matrices:

$$M=\begin{pmatrix} \overset{(2x2)}{M_1} & 0\ 0 \\ 0 & \overset{(4x4)}{M_2} \\ 0 & \end{pmatrix}, B=\begin{pmatrix} 0 & \overset{(2x2)}{B_1} & 0 \\ B_2 & \overset{(4x4)}{0} & \\ B_3 & & \end{pmatrix}, \qquad (6)$$

the system (5) can be rewritten, if M^{-1} exists, as:

$$(I-R)X=X_{(0)}, \qquad (7)$$

where $R=-M^{-1}B$ has the shape:

$$R=\begin{pmatrix} 0 & R_1 & 0 \\ R_2 & 0 & 0 \\ R_3 & 0 & 0 \end{pmatrix}, \qquad (8)$$

and where $X_{(0)}=M^{-1}S$. $X_{(0)}=(a_{(0)}^{(+1)},a_{(0)}^{(+2)},0,0,0,0)^T$ is the amplitude vector of the excitation coefficients of the plane waves generated by the source at the upper interface in the absence of the lower one. The elements of the matrix R: $R_1=-M_1^{-1}B_1$ and $(R_2\ R_3)^T=-M_2^{-1}(B_2\ B_3)^T$ may be interpreted as the matrix of reflection coefficients at the top free surface and the matrix of reflection-transmission at the coating-substrate interface respectively. Therefore the solution X is given by

$$X=(I-R)^{-1}X_{(0)}. \qquad (9)$$

The direct evaluation of $(I-R)^{-1}$ considers a wave coupling and thus the propagation problem is seen as a whole, with all possible interactions. In the context of a direct numerical inversion of both Laplace and Fourier transforms, it is rather difficult to integrate $(I-R)^{-1}X_{(0)}$ because it may have many poles for p and s_1 located on (or near) the paths of integration. Here we are going to deal with a series expansion of $(I-R)^{-1}$ for which each term of the series will be physically understandable in terms of mode conversion and wave travelling through the thickness of the layer [1]. This expansion is also known as the Debye's series expansion [2]. The operator $(I-R)^{-1}$ is expanded into power series of R as:

$$(I-R)^{-1}=I+R+R^2+R^3+\ldots \qquad (10)$$

Null coefficients in the R matrix implies that its even powers and odd powers retain the same structures:

$$R^{2k}=\begin{pmatrix} (R_1R_2)^k & 0 & 0 \\ 0 & R_2(R_1R_2)^{k-1}R_1 & 0 \\ 0 & R_3(R_1R_2)^{k-1}R_1 & 0 \end{pmatrix},$$
$$R^{2k-1}=\begin{pmatrix} 0 & (R_1R_2)^{k-1}R_1 & 0 \\ R_2(R_1R_2)^{k-1} & 0 & 0 \\ R_3(R_1R_2)^{k-1} & 0 & 0 \end{pmatrix}. \qquad (11)$$

Then the amplitude vector of down and up-going waves in the layer are respectively given by :

$$\begin{cases} a^{(+n)}=\sum_{k=0}^{\infty}\left[(R_1R_2)^k\right]_{nm}a_{(0)}^{(+m)} \\ a^{(-n)}=\sum_{k=0}^{\infty}\left[R_2(R_1R_2)^k\right]_{nm}a_{(0)}^{(+m)}e^{ps_3^{(-n)}h}, \end{cases} \qquad (12)$$

Those amplitudes are written in terms of a series of products of reflection coefficients at the interfaces with the corresponding phase terms. The product R_1R_2 represents a double vertical propagation through the thickness of the layer and k the number of such paths. For a fix value of k, we can collect terms in such a way that they are kinematic similar, that is with the same phase term, knowing that $s_3^{(-n)}=-s_3^{(+n)}$:

$$e^{-p(\alpha s_3^{(+1)}+\beta s_3^{(+2)})h}. \qquad (13)$$

This corresponds to the total vertical path length through the layer of a generalized-ray composed of α longitudinal and β transverse modes. The total amplitude of the whole set of rays of type $\alpha L\beta T$ including all the $(\alpha,\beta)!$ binomial combinations is:

$$\overline{a}_{(\alpha,\beta)}^{(\pm n)}=\sum^{(\alpha,\beta)!}\underbrace{r_{n\bullet}\ldots r_{\bullet m}}_{\alpha+\beta}a_{(0)}^{(+m)}, \qquad (14)$$

where the quantities r_{nm} are the reflection coefficients of a m-type wave converted into a n-type wave.

Therefore, each (α,β) contribution of the displacement field is given by:

$$\tilde{u}^{(+n)}_{i,(\alpha,\beta)}(x_3,s_1,p)=\bar{a}^{(+n)}_{(\alpha,\beta)}P^{(+n)}_i e^{-p(\alpha s_3^{(+1)}+\beta s_3^{(+2)})h}e^{-ps_3^{(+n)}x_3} \quad (15)$$

$$\tilde{u}^{(-n)}_{i,(\alpha,\beta)}(x_3,s_1,p)=\bar{a}^{(-n)}_{(\alpha,\beta)}P^{(-n)}_i e^{-p(\alpha s_3^{(+1)}+\beta s_3^{(+2)})h}e^{-ps_3^{(+n)}(h-x_3)}.$$

The coefficients r_{nm} are independent of the frequency p and the coefficients of excitation $a^{(+m)}_{(0)}$ are proportional to p^{-1}. The full solution is thus obtained by the sum of $\tilde{u}^{(\pm n)}_{i,(\alpha,\beta)}$ over all the values of (α,β).

Cagniard-de Hoop method

Performing the inverse Fourier transform with respect to the parameter s_1, the solution in the Laplace domain becomes:

$$\hat{u}^{(\pm n)}_{i,(\alpha,\beta)}(x_1,x_3,p)=\frac{p}{2i\pi}\int_{-i\infty}^{i\infty}\tilde{u}^{(\pm n)}_{i,(\alpha,\beta)}e^{-ps_1x_1}ds_1 . \quad (16)$$

The Cagniard-de Hoop method consists in collecting the phase terms in (16) and in defining a new variable τ such that [1]:

$$\begin{aligned}\tau&=(\alpha s_3^{(+1)}+\beta s_3^{(+2)})h+s_3^{(+n)}x_3+s_1x_1,\\ \tau&=(\alpha s_3^{(+1)}+\beta s_3^{(+2)})h+s_3^{(+n)}(h-x_3)+s_1x_1,\end{aligned} \quad (17)$$

respectively for down-going and up-going generalized-ray. This variable has the dimension of a time and is supposed to be real and positive. Then for each value of τ, α, β and for a specific n, there are two solutions for s_1 verifying Christoffel equation and equation (17). Those solutions can be real or complex conjugate. They define one Cagniard's path in the complex s_1 plane, which is parameterized by τ. There is one contour for each type of generalized-ray, according to the value of α and β and the nature, L or T, of the last converted ray reaching the point of observation. An example of such contours running in the complex plane of slowness may be found in [5].

The Cagniard's contours are symmetric with respect to the real s_1-axis. By closing the contours at infinity and by virtue of Cauchy's theorem, the integral taken over the original path $]-i\infty,i\infty[$ (16) is then equal to the integral taken over the Cagniard's contour running from $\mathrm{Im}(s_1)<0$ to $\mathrm{Im}(s_1)>0$. The influence of the branch points, the role of the branch cuts on the real axis and many other details on this deformation process can be found in Van der Hijden's book. Doing the change of variable $s_1\rightarrow\tau$ on the deformed integral, we get a new expression for (16):

$$\hat{u}^{(\pm n)}_{i,(\alpha,\beta)}(x_1,x_3,p)=\frac{1}{\pi}\int_{T_{arr}}^{+\infty}\mathrm{Im}(\bar{b}^{(\pm n)}_{(\alpha,\beta)}P^{(\pm n)}_i\partial_\tau s_1)e^{-p\tau}d\tau \quad (18)$$

where $\bar{b}^{(\pm n)}_{(\alpha,\beta)}(s_1)=p\bar{a}^{(\pm n)}_{(\alpha,\beta)}(s_1,p)$. T_{arr} is the time τ for which the Cagniard's contour leaves the real s_1 axis or the time at which the contour starts to run along the real branch cut in case of a head-wave. It defines the beginning of the time contribution of the ray. By immediate inspection we obtain the original of $\hat{u}^{(\pm n)}_{i,(\alpha,\beta)}$ in the time domain:

$$u^{(\pm n)}_{i,(\alpha,\beta)}(x_1,x_3,t)=\begin{cases}0, \text{ when } t<T_{arr}\\ \dfrac{1}{\pi}\mathrm{Im}(\bar{b}^{(\pm n)}_{(\alpha,\beta)}P^{(\pm n)}_i\partial_\tau s_1),\ T_{arr}<t\end{cases} \quad (19)$$

In order to get the full solution for the Green's function, we must add the contributions for all combinations (α,β) up to infinity. Obviously, knowing that each contribution is causal and begins at a specific time, for a given time window only a finite number of generalized-ray constituents are necessary.

Some examples of Green's functions

The thickness of the coating is $h=5\,\mathrm{mm}$ for all examples shown in this paper. The first one concerns a copper single crystal for which the axis x_3 is the crystallographic axis (100), overlaying an isotropic Nickel substrate. Copper crystal stiffness coefficients are, in GPa: $c^{(1)}_{11}=170$, $c^{(1)}_{13}=123$, $c^{(1)}_{55}=75.5$ and the mass density $\rho^{(1)}=8.93\,\mathrm{g.cm^{-3}}$. Nickel substrate properties are: $c^{(2)}_{11}=324$, $c^{(2)}_{55}=80$ and $\rho^{(2)}=8.905\,\mathrm{g.cm^{-3}}$. Figure 2 shows the displacement field at a point on the surface. All singularities in the Green's function correspond to wave arrivals predicted by geometrical acoustics. If bulk-wave arrivals are easily recognized as singularities in the Green's function, for other types of features such as head-waves (and their multiple reflections), ray-focusing (internal diffraction), it may be more intricate to see and analyze their signature. But one must remember that those waveforms stem from sums of different generalized-rays which can easily be characterized by their corresponding wave constituents and related contours in the complex plane.

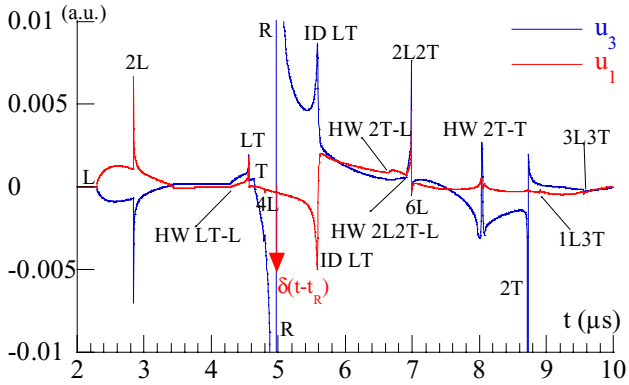

Figure 2: displacement field at $x_1=10\,\mathrm{mm},x_3=0\,\mathrm{mm}$

Labels in figure 2 indicate type of feature: 2L2T for bulk-wave arrival after two paths of L-type ray and two others of T-type through the layer ; HW LT-L means head wave contribution composed of one L and one T-type ray within the layer and a L-type grazing ray in the substrate ; and ID LT is related to internal

diffraction sharp (but not singular) contribution conveyed after one mode conversion L-T. Multiple head-wave reflection is exemplified in figure 3-a which shows impulse response at the surface for larger horizontal offset. The fact that longitudinal waves propagate much faster in the nickel half-space than in the copper layer allows the formation of several types of head-wave fronts arriving earlier than the first reflected bulk-waves. Convolution of the Green's function with a gaussian pulse (see figure 3-b) gives a measure of the amplitude of such fronts compared to amplitude of first few bulk-waves. Here, the amplitude of the first head-wave detected is about 20 times less than the amplitude of direct L-wave but its early signal is well separated in time, which is its main interest in material characterization.

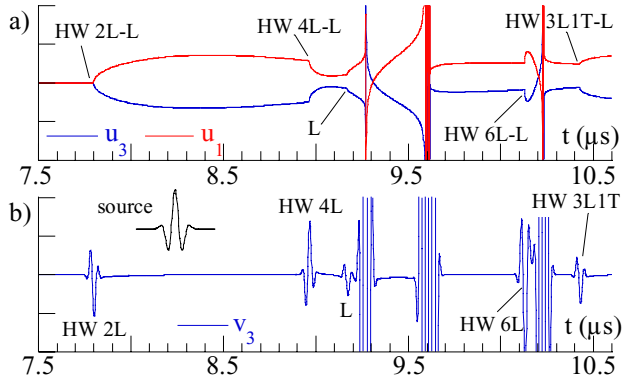

Figure 3: Head-waves at $x_1 = 40\,\text{mm}$, $x_3 = 0\,\text{mm}$. Green's function for displacement (a) and vertical component of particle velocity after convolution (b).

Wave field decomposition into generalized-ray constituents is an interesting way of analyzing in the time domain wave interaction with interfaces. As an example, consider upper surface response for which a singularity appears at the Rayleigh wave arrival (figure 4). Despite the fact that there is strictly speaking no Rayleigh wave propagating at the free upper surface (vacuum/copper interface) due to the presence of the second interface, in the time domain, as long as transient field has not yet interacted with the interface separating the coating from the substrate, the surface response is given by the Green's function of the copper medium seen as an half-space. With distance away from the source and time increasing, the perturbation of Rayleigh wave field due to the substrate may be analyzed via the contributions brought by the generalized-rays series (see figure 4).
Exact Green's function obtention and its good understanding via Cagniard technique is for sure at the expense of a certain numerical implementation effort. Just in view of quantitative comparison with purely numerical approach, figure 5 shows the superposition with the standard (ω,k) integration method [6] which is somehow simpler to compute while it reaches a very good accuracy.

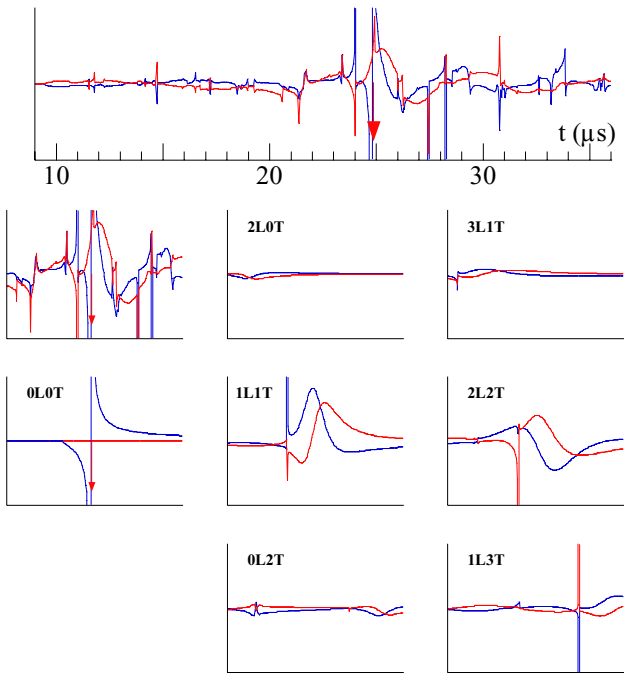

Figure 4: Decomposition into generalized-ray constituents about Rayleigh wave arrival at $x_1 = 50\,\text{mm}$, $x_3 = 0\,\text{mm}$.

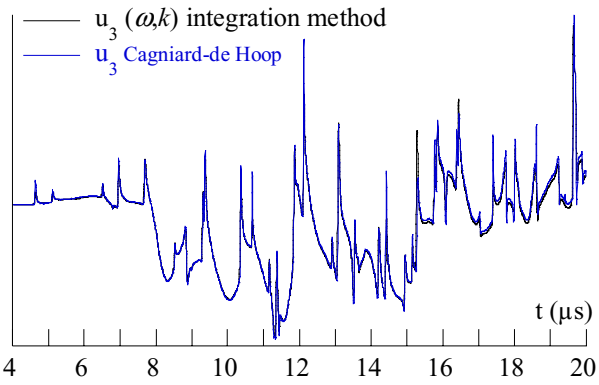

Figure 5: Comparison between Cagniard-de Hoop technique and (ω,k) integration method for a copper plate at $x_1 = 20\,\text{mm}$, $x_3 = 5\,\text{mm}$.

References

Book:

[1] J. H. M. T. Van Der Hijden, Propagation of transient elastic waves in stratified anisotropic media, Elsevier Science Publishers,vol. 32, 1987.

Transaction, Proceedings or Journal Articles:

[2] M. Deschamps and P. Chevée, Wave Motion, Vol. 15, p. 61, 1992.

[3] M. R. Hauser, R. L. Weaver and J. P. Wolfe, Phys. Rev. Lett. 68, p. 2604, 1992.

[4] A. G. Every, Phys. Rev. B 24, p. 3456, 1981

[5] O. Poncelet, M. Deschamps, A.G. Every, IEEE UFFC-WCU, p. 619, Atlanta, october 7-10, 2001.

[6] B. Audoin, H. Meri, 5th WCU, Paris, september 7-10, 2003.